

Deconfined quantum criticality in the two dimensional Antiferromagnetic Heisenberg model with next nearest neighbour Ising exchange

J. Hove and A. Sudbø

Department of Physics, Norwegian University of Science and Technology, N-7491 Trondheim, Norway

(Dated: July 9, 2018)

We have considered the $S = 1/2$ antiferromagnetic Heisenberg model in two dimensions, with an additional Ising next-nearest neighbour interaction. Antiferromagnetic next-nearest neighbour interactions will lead to frustration, and the system responds with flipping the spins down in the xy plane. For large next nearest neighbour coupling the system will order in a striped phase along the z axis, this phase is reached through a first order transition. We have considered two generalizations of this model, one with random next-nearest neighbour interactions, and one with an enlarged unit cell, where only half of the atoms have next-nearest neighbour interactions. In both cases the transition is softened to a second order transition separating two ordered states. In the latter case we have estimated the quantum critical exponent $\beta \approx 0.25$. These two cases then represent candidate examples of deconfined quantum criticality.

PACS numbers: 75.10.Jm, 75.10.Nr, 75.40.Mg, 75.40.Cx

I. INTRODUCTION

The groundstate of the antiferromagnetic Heisenberg model is macroscopically degenerate. This makes it particularly sensitive to additional interactions, which might induce transitions to different states[1]. In a seminal paper the concept of fractionalized order, was set forth in Ref. [2]. The generic starting point of this analysis is the two dimensional antiferromagnetic Heisenberg model

$$H = J \sum_{\langle i,j \rangle} \vec{S}_i \cdot \vec{S}_j + \dots, \quad (1)$$

where the ellipsis represent additional short range interactions, governed by a coupling g . For $g = 0$ the groundstate is the antiferromagnetic Néel state, and by tuning g the system can supposedly be driven through a continuous quantum phase transition to a state with a different type of order. According to the Landau-Ginzburg-Wilson (LGW) paradigm for phase transitions, an order-to-order transition must either be first order, or proceed via an intermediate disordered state. Since the scenario envisaged in Ref. [2], namely a *continuous* order-to-order transition, breaks with this paradigm, the term “deconfined criticality” was coined to describe these transitions [2].

The only microscopic model considered in some detail in the context of deconfined criticality is a dimer model with two spins in the unit cell[3]. For this particular model the transition between a Néel state and a spin-gapped paramagnet can be shown analytically, and are also confirmed with QMC calculations[4]. Apart from this dimer model it has been difficult to construct microscopic models which give rise to deconfined criticality. Sandvik et.al. have investigated a model with ferromagnetic XY interactions and a four-spin ring exchange[5, 6], this model has a quantum critical point separating a superfluid and valence bond solid, which might be a microscopic manifestation of deconfined criticality. Another possible way to build a microscopic model which might

give rise to deconfined criticality is to include frustration. A natural way to frustrate the Heisenberg model is with a next nearest neighbour (nnn) Heisenberg interaction; this is usually called the $J_1 - J_2$ model. The J_2 coupling will favor antiparallel spins along next nearest neighbour bonds, this is in conflict with the nearest neighbour exchange. The result is frustration, and a reduction in the antiferromagnetic ordering.

Unfortunately, in this model the geometric frustration gives rise to a sign-problem, and the model is really not amenable to a Monte Carlo based approach. Studies of this model have been based on a reweighting technique[7], exact diagonalization[8] and variational methods[9]. The results indicate that Néel order persists up to $\kappa = J_2/J_1 \lesssim 0.40$, and that a striped order develops for $\kappa \gtrsim 0.60$. Recent results indicate that the transition at $\kappa \sim 0.40$ is a weak first-order transition[10].

To avoid the sign problem of the $J_1 - J_2$ model, one can study a simplified model where the nnn exchange is only along the z -components of the spin, i.e. the model

$$H = J \left(\sum_{\langle i,j \rangle} \vec{S}_i \cdot \vec{S}_j + \kappa \sum_{\langle\langle i,j \rangle\rangle} S_i^z S_j^z \right). \quad (2)$$

This simplified model captures the effect of frustration, but in contrast to the $J_1 - J_2$ model the isotropy in spin space is explicitly broken by the next-nearest neighbour interaction. Hence, in particular for small κ we expect this to be a much stronger perturbation of the antiferromagnet Heisenberg model than the J_2 coupling.

Apart from the Heisenberg point at $\kappa = 0$ we expect three different phases as κ is varied: For $\kappa < 0$ the system is not frustrated, and the additional next-nearest neighbour will only serve to increase the antiferromagnetic ordering. Observe however that the next-nearest neighbour interaction has singled out the z direction in spin space, i.e. the model should be in the universality class of the Ising model and have an ordered state at finite T . For $\kappa > 0$ the system will be frustrated, for

moderate κ we expect that the system will avoid the frustration by flipping the spins down in the xy plane, i.e. we will effectively get an antiferromagnetic $O(2)$ model. For larger values of κ the next-nearest neighbour interaction will dominate, in which case the spins will again point along the z axis, and order in a state with stripe order. The transition from the effective antiferromagnetic $O(2)$ model to the striped state is first order. In Ref. [11] an antiferromagnetic Heisenberg model with an additional *anisotropic* next-nearest neighbour exchange was studied. This work reported Monte Carlo results in the limit of zero transverse nnn interactions; i.e. Eq. 2. In addition, a model similar to Eq. 2 in the terms of hardcore bosons was considered in Refs. [12, 13]. We have determined the phase diagram of Eq. 2, essentially reproducing the results of Refs. 11, 12, 13. In addition, we have considered two generalisations aimed at softening the first order transition to the striped state.

The generalisations of Eq. 2 we have considered are first a disordered model, where the next-nearest neighbour bond strength is $\kappa_0 \pm \Delta\kappa$ with equal probability. This is motivated from a theorem [14] which states that in two dimensions any amount of bond disorder will be sufficient to soften a first order transition into a second order transition. Secondly, we have studied a model where only half of the sites have next-nearest neighbour interaction. This model will clearly share many of the qualitative features of the original model, but the effect of the next-nearest neighbour interactions will be reduced.

II. QMC SIMULATIONS

We have performed Quantum Monte Carlo simulations using the Stochastic Series Expansion (SSE)[15, 16] method. In the SSE method the Hamilton operator is written as a sum of bond operators

$$H = \sum_b (H_{d,b} + H_{od,b}). \quad (3)$$

The sum in Eq. 3 is over all the bonds on the lattice, $H_{d,b}$ is an operator working on bond b , which is *diagonal* in the basis chosen to represent the spin space, and $H_{od,b}$ is an off-diagonal operator. For spin models with z axis magnetization as basis, the operator $H_{d,b}$ will be

$$H_{d,b} = J S_{i(b)}^z S_{j(b)}^z, \quad (4)$$

where $i(b)$ and $j(b)$ are the two sites connected by bond b . $H_{od,b}$ is an off-diagonal operator, and in the case of spin models we will have $H_{od,b}$ given by

$$H_{od,b} = \frac{J}{2} (S_{i(b)}^+ S_{j(b)}^- + S_{i(b)}^- S_{j(b)}^+). \quad (5)$$

Observe that for the actual simulations the operators $H_{d,b}$ are scaled and shifted[16] to ensure

$$H_{d,b} |\uparrow\downarrow\rangle = |\uparrow\downarrow\rangle \quad H_{d,b} |\uparrow\uparrow\rangle = 0. \quad (6)$$

The formal expression for the partition function is then expanded, which yields the following representation

$$Z(\beta) = \sum_{\{\alpha\}} \sum_n \sum_{\{S_n\}} \frac{(-\beta)^n}{n!} \left\langle \alpha \left| \prod_i^n H_{\sigma_i} \right| \alpha \right\rangle. \quad (7)$$

Here S_n is a sequence of n pairs, each pair consisting of a variable denoting operator type and a bond index, i.e.

$$S_n = \left\{ \underbrace{(a_1, b_1)}_{\sigma_1}, (a_2, b_2), \dots, (a_n, b_n) \right\}. \quad (8)$$

The variable a_i in Eq. 8 denotes *type* of operator and can be either diagonal or off-diagonal. The SSE method then consists of doing importance sampling in the combined space $|\{\alpha\}\rangle \otimes S_n$. The actual updates are of two different types. The diagonal updates insert or remove a diagonal operator $H_{d,b}$, thereby changing the expansion order $n \rightarrow n \pm 1$. The off-diagonal operators change operator types $H_{d,b} \leftrightarrow H_{od,b}$ and flip the corresponding spins, this must be done in a way which ensures periodicity in the β direction, i.e. $|\alpha(0)\rangle = |\alpha(n)\rangle$. For the off diagonal updates, the advent of loop updates [17] has significantly improved the performance of SSE simulations [18, 19].

For the ordinary $S = 1/2$ Heisenberg model, SSE simulations with operator loop update are particularly simple. In order to include the next-nearest neighbour interactions, we need to modify the algorithm slightly. In the case of the diagonal updates this merely amounts to including the extra factor κ in the weight calculation for the next-nearest neighbour bonds. Whereas for the operator loop the next-nearest neighbour interactions have a more profound effect. These interactions are *only* diagonal, i.e. the incoming and outgoing spin states must be equal. Furthermore, the next-nearest neighbour bonds can only connect antiparallel ($\kappa > 0$) spins. The result of this is that the next-nearest neighbour bonds “freeze” a substantial part of the spin configuration, and only those spins/operators not directly linked to a next-nearest neighbour bond are amenable to operator loop update, as illustrated in Fig. 1. Clearly, this freezing affects the performance of the simulations in a negative way, in particular for intermediate values of κ .

A. Observables

To differentiate between the different types of order in the model, we have studied the structure factor

$$S(\mathbf{Q}) = \frac{1}{N} \left\langle \left(\sum_{\mathbf{r}} \langle \alpha | S^z(\mathbf{r}) | \alpha \rangle e^{i\mathbf{Q}\cdot\mathbf{r}} \right)^2 \right\rangle, \quad (9)$$

for different values of \mathbf{Q} . An estimator of $S(\mathbf{Q})$ taking all the intermediate SSE states into account can be found in [16]. For the remaining part of the text we will make

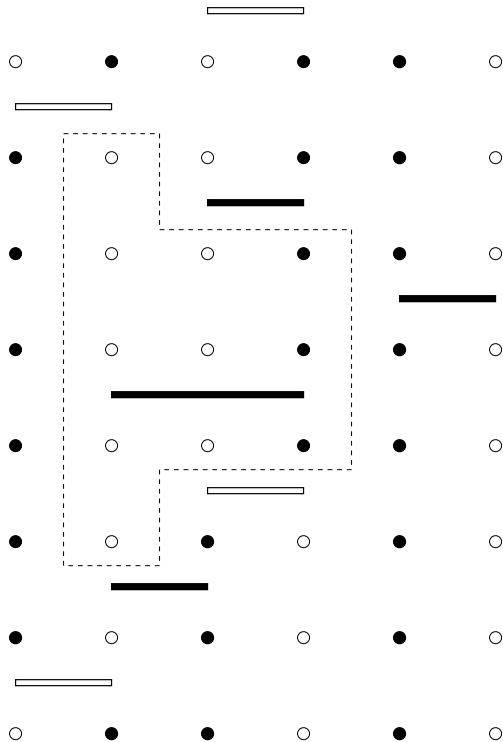


FIG. 1: A chain of six spins, depicted with an operator sequence of length $n = 8$ in the β direction. The filled bars denote diagonal interactions $S_i^z S_j^z$ and the open bars are flip operators $S_i^+ S_j^- + S_i^- S_j^+$. The dashed region shows spins/p-slices which have been frozen by the next-nearest neighbour bond in the middle.

frequent use of the terms staggered and striped magnetization, these quantities are defined as

$$M_{(\pi,\pi)}^z = \frac{1}{N} \sqrt{3S(\pi,\pi)}, \quad (10)$$

$$M_{(\pi,0)}^z = \frac{1}{N} \sqrt{S(\pi,0) + S(0,\pi)}. \quad (11)$$

The upper index indicates that the magnetization is evaluated along the z axis, and the lower index is the direction of \mathbf{Q} in the evaluation of Eq. 9, i.e. (π, π) for staggered and $(\pi, 0)$ for striped magnetization. The factor of three in Eq. 10 is included to account for rotational averaging among the three directions in spin space. When κ is finite, isotropy in spin space is explicitly broken. We have nevertheless retained this factor to get continuous formulae around $\kappa = 0$. In addition to the structure factor, we have also measured two other quantities, namely specific heat and superfluid density.

The specific heat is given by

$$C_V = \beta^2 \frac{\partial^2}{\partial \beta^2} \ln Z = \langle n(n-1) \rangle - \langle n \rangle^2. \quad (12)$$

Here, n refers to the summation variable in Eq. 7. This summation is truncated in a stochastic manner and n is thus promoted to a dynamical variable in SSE. We

will not exhibit results for C_V explicitly, but have used the anomalies in this quantity to corroborate the phase boundaries shown in Fig. 4 (with the exception of the line separating the superfluid phase from the disordered phase, see comments on this below).

The estimator for the superfluid density ($O(2)$ ordering) is given by [16]

$$\rho_S = \frac{3}{4\beta N} \left(\langle (N_x^+ - N_x^-)^2 \rangle + \langle (N_y^+ - N_y^-)^2 \rangle \right), \quad (13)$$

where N_μ^+ / N_μ^- is the number of $S_i^+ S_j^-$ and $S_i^- S_j^+$ operators applied along bonds in the μ direction.

III. RESULTS

As mentioned previously, the model in the form of Eq. 2 has already been studied in Ref. [11]. As a benchmark of our QMC methods, we started with this model to reproduce the results of Ref. [11]. Figs. 2 and 3 shows the staggered and striped magnetization along the z axis, as a function of κ .

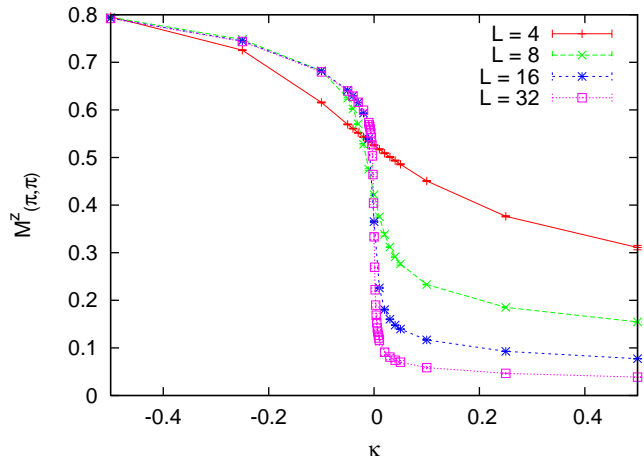


FIG. 2: (Color online) The staggered magnetization along the z axis in the ground state ($\beta = 10$), as a function of κ .

From these two figures we conclude the following. (1) For negative κ the magnetization along the z axis is enhanced; this is expected since the $\kappa < 0$ system is not frustrated. (2) For $\kappa \gtrsim 0$ the magnetization is immediately tilted away from the z axis, leaving zero magnetization along the z axis. (3) For large κ the magnetization again orders along the z axis, in this case in a striped formation. The transition to the striped phase is a first order transition, the discontinuous jumps in $M^z(\pi, 0)$ in Fig. 3 indicate this, and it is also confirmed by a more detailed analysis of histograms of e.g. the striped order parameter[11] or number of next-nearest neighbour bond operators. Hence, for this case the order-to-order transition depicted in Fig. 3 (a transition from superfluid order, equivalently $O(2)$ order, to stripe order) falls

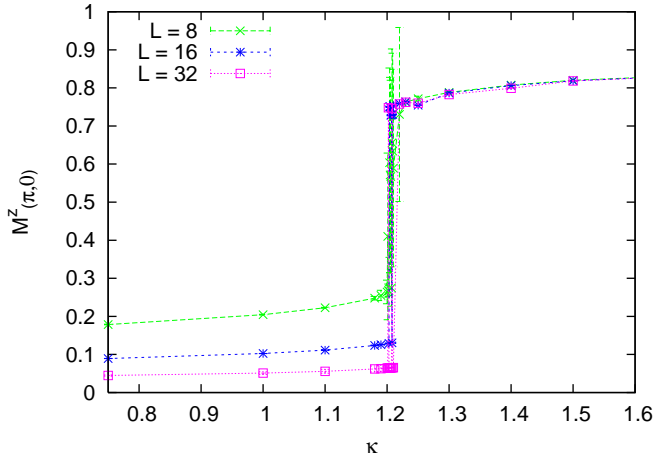


FIG. 3: (Color online) The striped magnetization in the ground state ($\beta = 10$), as a function of κ . There is a first order transition at $\kappa \approx 1.205$.

within the standard Landau-Ginzburg-Wilson paradigm of phase transitions.

For $\kappa < 0$ and $\kappa > 0$ the ordered state breaks a discrete symmetry, and the order persists for finite T . In the intermediate regime, $0 < \kappa \lesssim 1.205$ the remaining model is an antiferromagnetic $2DXY$ model with a continuous $O(2)$ symmetry. According to the Mermin-Wagner theorem this symmetry can not be spontaneously broken at finite T . However, there is finite spin stiffness and topological order up to a temperature T_{BKT} where the order vanishes in a *Berezinski-Kosterlitz-Thouless* transition. The boundary of this region has been (approximately) located by equating $\rho_S(T)$ with $2T/\pi$. All in all we have found the phase diagram presented in Fig. 4 for Eq. 2.

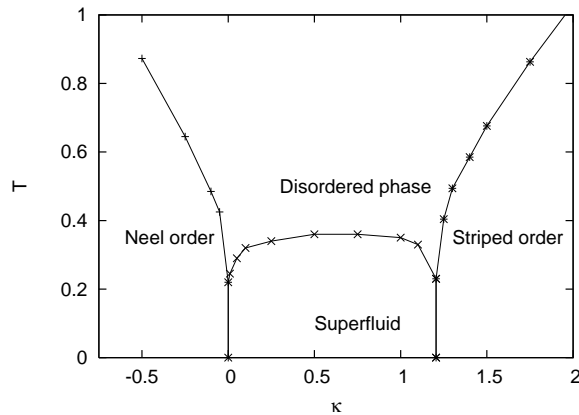


FIG. 4: Phase diagram for the model in the κ, T plane. For $\kappa > \kappa_c$, and $\kappa < 0$ the model has magnetic order, striped and staggered respectively. In the intermediate κ range values there is no finite T magnetic order, however there is a superfluid order which persists into the finite T region. The line separating topological $2DXY$ order from the normal phase is determined with considerably less precision than the two other lines.

A. Disordered system

The effect of disorder on phase transitions is a much studied topic. In the case of continuous transitions, the Harris criterion [20, 21] states that disorder will change the universality class of the transition, i.e. be relevant, if the exponents of the pure system satisfy $\nu < 2/d$. In the case of first order transitions, disorder can soften the transition into a continuous transition, in the case of two dimensions any amount of disorder is sufficient [14], whereas a finite amount is needed in three dimensions. These predictions have been confirmed for the Potts model in both two and three dimension [22, 23]. We have, however, not found tests of these predictions for a first order *quantum* phase transition. We have investigated what happens with the first order quantum phase transition at $\kappa \approx 1.205$ when disorder is included in the model. Along each bond is κ is given by

$$\kappa = \kappa_0 \pm \Delta\kappa, \quad (14)$$

with equal probability. We have focused on the striped order parameter $M^z(\pi, 0)$ in the vicinity of $\kappa \approx 1.205$, in order to compare with Fig. 3. In the disordered system we must perform both ordinary thermodynamic averaging and subsequently disorder averaging. In e.g. Fig. 5 the plotted quantity is given by

$$\overline{M^z(\pi, 0)} = \frac{1}{N} \sum_{i=1}^N M_i^z(\pi, 0), \quad (15)$$

where $M_i^z(\pi, 0)$ is the striped magnetization in disorder realization i , calculated according to Eq. 11, and N is the total number of disorder realizations. The number of disorder realizations has typically been $N = 100$.

Fig. 5 shows the disorder averaged striped magnetization as a function of κ_0 for $\Delta\kappa = 0.05$. The strongly discontinuous features of $M^z(\pi, 0)$ from Fig. 3 are washed out when disorder is introduced. From this, we conclude that the transition changes order when disorder is introduced. The location of the critical point coincides with the original transition point of the uniform system. We have not varied $\Delta\kappa$ systematically, our results (not shown) indicate that the system is not very sensitive to $\Delta\kappa$ variations.

The low- κ region in Fig. 5 is an $O(2)$ ordered state. The large- κ region is an Ising-ordered state with an additional stripe order. Hence, this quantum phase transition is a transition from an ordered state to another ordered state, and since it is continuous, it represents a candidate example of so-called *deconfined quantum criticality*.

B. AB system

For large κ the Ising next-nearest neighbour interaction in Eq. 2 is a very strong interaction. In an attempt

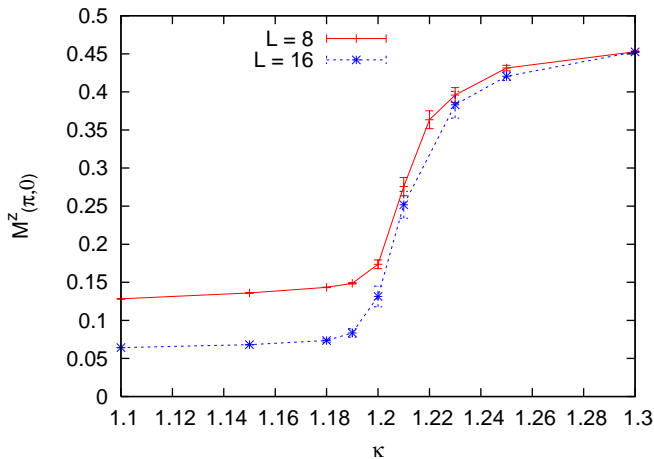


FIG. 5: (Color online) Disorder averaged value of $M^z(\pi, 0)$ as a function of κ_0 for two different system sizes. The indicated error bars are standard error estimates from the independent disorder realizations. The temperature coupling is $\beta = 10$.

to soften the transition to the high κ state into a continuous transition we have devised a model consisting of two “atom” types A and B, where the Ising next-nearest neighbour interaction is only between the A atoms, the scenario is illustrated in Fig. 6.

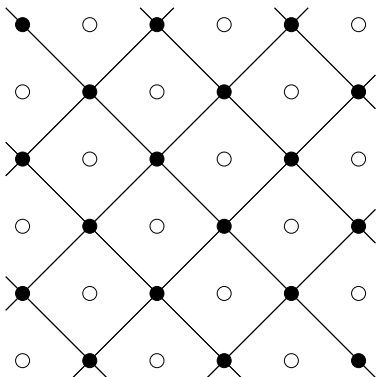


FIG. 6: The binary system consisting of two different atomic species. Only type A (●) has next-nearest neighbour interaction, illustrated with diagonal lines.

This model has many of the same qualitative properties as the original model, in particular small values of κ will frustrate the system and tilt the magnetization down in the xy plane. For large κ the A atoms will form an antiferromagnetically ordered state, with AF magnetization along the z axis. In this state the A and B sites will decouple, and the B sites will be disordered with no net contribution to the energy of the system. As an order parameter for this transition we have considered the staggered magnetization along the z axis, for the A sites, i.e.

$$M^z_{(\pi/2, \pi/2)} = \frac{1}{N} \sqrt{S_A(\pi/2, \pi/2)}, \quad (16)$$

where the sum is only over A sites. Because the sum is limited to the A sites, full polarization corresponds to $M^z = 0.25$. Fig. 7 shows the staggered magnetization among the A sites as a function of κ .

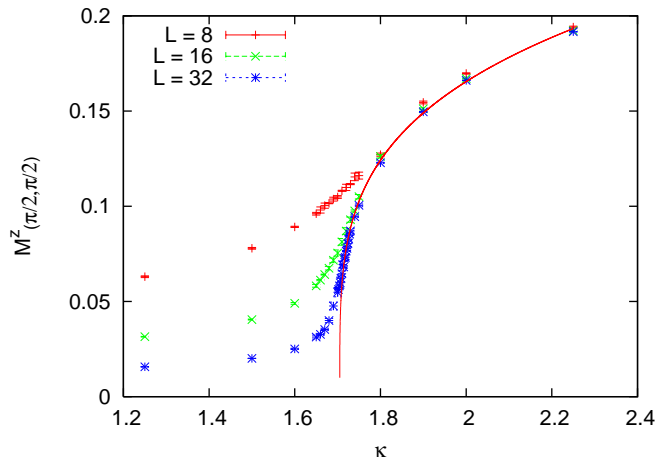


FIG. 7: (Color online) The staggered magnetization of the A sites in the groundstate of the AB model, as a function of κ . The solid line is a least squares fit to a power law.

Comparing with the striped magnetization of the uniform model, Fig. 3, we see that the critical coupling $\kappa_c \approx 1.705$ of the AB system is much larger than for the uniform system. This is reasonable, since the next-nearest neighbour interaction only operates on half of the sites. Furthermore, Fig. 7 shows that the transition to the ordered state is much smoother than in the uniform model, hence the figure indicates that the transition is continuous. The continuous nature of the transition is also confirmed by considering the number distribution of e.g. next-nearest neighbour operators at critical point. This quantity is unimodal, whereas for the uniform model it is strongly bimodal, reminiscent of a first order transition. From this, we conclude that the AB-model deformation of the Hamiltonian in Eq. 2 suffices to promote quantum deconfined criticality. Stripe order is lost by removing every second next-nearest neighbor coupling, but an order-to-order quantum phase transition nevertheless remains. Namely, the transition is that from an $O(2)$ (superfluid) ordered state at low and intermediate values of κ to a Z_2 (Ising) ordered state at high values of κ . *Since the transition is second order, it represents a second candidate example of deconfined quantum criticality.*

We have not made attempts at completely determining the critical exponents at the transition. However a fit of M^z from the $L = 32$ system to the functional form

$$M^z_{(\pi/2, \pi/2)} \propto |\kappa - \kappa_c|^\beta \quad (17)$$

with $\kappa_c = 1.705$ gave good results, with a critical exponent $\beta \approx 0.25$. The fit is shown as a solid line in Fig. 7.

IV. CONCLUSION

We have studied varieties of the antiferromagnetic Heisenberg model in two dimensions with additional next-nearest neighbour Ising exchange. This model has a strong first order transition at $\kappa_c \approx 1.205$. We have studied two generalisations of the model, one based on disordered next-nearest neighbour couplings, and another where only half the sites are endowed with next-nearest neighbour interaction. Both the generalised models feature continuous quantum phase transitions from one ordered state to another ordered state. *As such, these two cases represent candidate examples of deconfined quantum criticality.* Frustrated interactions is an essential

part of the models we have considered, and as such they are distinct from the model already considered by Sandvik et.al. [5, 6], where (possible) deconfined criticality is brought about by ring-exchange.

V. ACKNOWLEDGEMENT

This work was supported in part by the Research Council of Norway through Grants No. 157798/432 and 158547/431 (NANOMAT) and 167498/V30(STORFORSK). Bergen Center for Computational Science (BCCS) is acknowledged for computing time.

-
- [1] A. Cuccoli, T. Roscillo, V. Tognetti, R. Vaia, and P. Verucchi, Phys. Rev. B **67**, 104414 (2003).
 - [2] T. Senthil, A. Vishwanath, L. Balents, S. Sachdev, and M. P. A. Fisher, Science **303**, 1490 (2004).
 - [3] S. Sachdev, *Quantum magnetism* (Springer, 2004), chap. Quantum phases and phase transitions of Mott insulators.
 - [4] M. Matsumoto, C. Yasuda, S. Todo, and H. Takayama, Phys. Rev. B **65**, 014407 (2001).
 - [5] A. W. Sandvik, S. Daul, R. R. P. Singh, and D. J. Scalapino, Phys. Rev. Lett. **89**, 247201 (2002).
 - [6] R. G. Melko, A. W. Sandvik, and D. J. Scalapino, Phys. Rev. B **69**, R100408 (2004).
 - [7] T. Nakamura and N. Hatano, Journal of the Physical Society of Japan **62**, 3062 (1993).
 - [8] H. J. Schulz, T. A. L. Ziman, and D. Poilblanc, J. Physique I **6**, 675 (1996).
 - [9] L. Capriotti, F. Becca, A. Parola, and S. Sorella, Phys. Rev. Lett. **87**, 097201 (2001).
 - [10] J. Sirker, Z. Weihong, O. P. Sushkov, and J. Oitmaa, cond-mat (2006).
 - [11] T. Roscilde, A. Feiguin, A. L. Chernyshev, S. Liu, and S. Haas, Phys. Rev. Lett. **93**, 017203 (2004).
 - [12] F. Hébert, G. G. Batrouni, R. T. Scalettar, G. Schmid, M. Troyer, and A. Dorneich, Phys. Rev. B **65**, 014513 (2001).
 - [13] G. Schmid and M. Troyer, Phys. Rev. Lett. **93**, 067003 (2004).
 - [14] M. Aizenman and J. Wehr, Phys. Rev. Lett. **62**, 2503 (1989).
 - [15] A. W. Sandvik and J. Kurkijärvi, Phys. Rev. B **43**, 5950 (1991).
 - [16] A. W. Sandvik, Phys. Rev. B **56**, 11678 (1997).
 - [17] H. G. Evertz, G. Lana, and M. Marcu, Phys. Rev. Lett. **70**, 875 (1993).
 - [18] A. W. Sandvik, Phys. Rev. B **59**, R14157 (1999).
 - [19] O. F. Syljuåsen and A. W. Sandvik, Phys. Rev. E **66**, 046701 (2002).
 - [20] J. T. Chayes, L. Chayes, D. S. Fisher, and T. Spencer, Phys. Rev. Lett. **67**, 2999 (1986).
 - [21] A. B. Harris, J. Phys. C **7**, 1671 (1974).
 - [22] S. Chen, A. M. Ferrenberg, and D. P. Landau, Phys. Rev. B **52**, 1377 (1995).
 - [23] C. Chatelain, B. Berche, W. Janke, and P.-E. Berche, Nucl. Phys B **719/3**, 275 (2005).